Version of Record: https://www.sciencedirect.com/science/article/pii/S0306261918317641
Manuscript_b6a97df5afec57046393047150a07b8b

Seismic response of offshore wind turbine with hybrid monopile foundation based on centrifuge modelling

Xuefei Wang, Xiangwu Zeng, Xu Yang, Jiale Li*
Department of Civil Engineering, Case Western Reserve University,
10900 Euclid Avenue, Bingham Building Room 208, Cleveland, OH, 44106

Corresponding author email: xxw165@case.edu.

Abstract: Some large capacity offshore wind turbines are constructed in seismically active areas. The occurrence of soil liquefaction during an earthquake can result in severe failures of the offshore wind turbine. The seismic response of the structure and the failure mechanism of the soil-structure interactions are necessary to investigate. In this study, the seismic response of an innovative hybrid monopile foundation is investigated through a series of centrifuge tests. The seismic performance of the combined system of the superstructure, foundation, and soil are demonstrated. Five hybrid foundation models are tested by considering the influence of the foundation thicknesses and diameters, and a monopile foundation is tested for comparison. Centrifuge test results reveal that the hybrid monopile foundation is effective in reducing the lateral displacement during the shaking. In the saturated condition, soil keeps its strength and stiffness beneath and adjacent to the foundation. The hybrid foundation system tends to settle more due to the larger shear stress caused by the soil structure interactions. Influences of the wheel specifications are illustrated. The foundations with larger thicknesses lead to smaller lateral displacements and lower tendencies of liquefaction, but the settlements are intensified. The larger diameter foundation provides a longer drainage path for the excess pore water pressure. With a similar weight, the structure settles less during the earthquake.

Keywords: Centrifuge modelling; earthquake loading; hybrid monopile foundation; lateral failure; optimized design; settlement.

1. Introduction

The offshore wind industry experiences rapid growth in recent years [1]. Normally, wind resources in offshore areas are stronger and more uniform. The electrical output is about 1.7 times compared to the onshore wind turbine with the same capacity [2, 3]. The onshore wind farms are required to locate at the sites with high wind speeds, but the appropriate locations are scarce due to the limitation of available lands and disturbances to human lives [4, 5]; on the contrary, the offshore wind resource is plentiful, and the available construction sites are abundant [6, 7]. In order to get better energy production and lower the capital cost, the size of a wind turbine is growing continuously [8, 9]. Meanwhile, there is a tendency that the offshore wind farm is built at locations with deeper water depths and further distances to shorelines [10]. In

Europe, the average water depth for newly installed wind farms is 27.5m, and the average distance to the land is 41km, which is 1.5 times and 3 times of those in 2009, respectively [11]. The environmental conditions at offshore wind sites are more complex considering combined loadings; thereby, the design criteria for onshore wind turbines cannot be applied directly. Currently, the evolution of the site selection further complicates the design and construction of the offshore wind turbines (OWTs). The unpredictable weather conditions lead to more challenges to ensure the in-situ structural stability. Therefore, investigations of the bearing behavior of OWTs under complex environmental conditions are necessary for the offshore wind industry.

The OWT is a slender structure with a large height (H)/width (W) ratio. Besides the self-weight, the structure should sustain ultimate or cyclic lateral loadings caused by wind, wave, and ice. These lateral loadings are applied at the upper structure and transmitted to the foundation, leading to large total overturning moments to the support structure [12, 13]. The tilting is the predominant failure of an OWT [14]. In an offshore wind project, the fabrication, transportation, and installation of the foundation part account for 30% to 50% of the total cost [15]. Therefore, bearing behavior of the support structure for OWT requires thorough and innovative investigations by considering the variable loading conditions. To date, the most widely used support structure for OWTs is the monopile foundation, accounting for 87% of the installed wind farms in Europe with a total number of 3720. The total number of gravity base supported OWT is 283, which contributes 6% of the market share [11]. A significant number of investigations have been conducted to study the bearing mechanism of these two substructures, and the design standards have been put forward [16]. With the development of larger capacity wind turbines and the more unpredictable environmental conditions, traditional substructures start to show their limitations. The diameter of the monopile foundation becomes much larger in deeper water, which significantly increases the material cost and the installation cost. The gravity base will turn to be excessively large, which may bring challenges for the construction and installation [17]. Therefore, studies of innovative substructures are necessary for future development.

The concept of the hybrid monopile foundation is proposed to fulfill the current requirements of OWTs (Figure 1). It is a combination of the traditional monopile foundation and the gravity base, which is more suitable for supporting the combined lateral and vertical loadings associated with the OWT while maintaining the simplicity of the design by adopting established design methods. The monopile is reinforced by a friction wheel located at the soil surface. The interactions between the two components provide a positive effect on the overall bearing capacity of the innovative foundation. This concept is initiated by the concept of pile caps and embedded retaining wall with stabilizing platforms [18, 19]. The ultimate bearing behavior of the hybrid monopile foundation has been investigated in our laboratory through a set of centrifuge tests, and three analytical methods are put forward in estimating its bearing capacity, including the “add-up method”, the “equivalent moment method”, and “direct calculation method” [20, 21]; the response in service conditions have been studied afterward, and the accumulated lateral displacement is predicted [22]. A similar concept, piled footing, has been investigated through

tests and numerical analysis; it is demonstrated that the footing effectively reduces the moment applied on the monopile [23]. Arshi [24] studies the bearing behavior of the monopiled footing foundation under lateral loadings and summarizes a design chart according to analytical and numerical results. It is illustrated that the footing size has a significant influence on the overall bearing capacity. For a given pile diameter and length, increasing the footing diameter tends to increase the lateral bearing capacity.

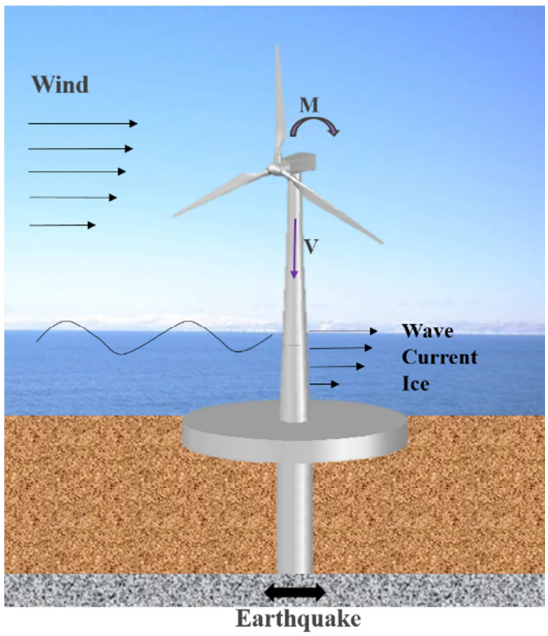

Figure 1. Schematic of OWT with hybrid monopile foundation

Some of the offshore wind farms are built in seismic active areas. To ensure the stability of wind turbines in service conditions, investigations of the seismic response are necessary, which reveals the failure mode of OWTs under the earthquake condition and provides an effective method in the remediation. At offshore areas where the soil deposits are saturated, the strong shaking may result in soil liquefactions. The generation of the excess pore water pressure softens the soil, leading to the reduction of soil bearing capacity. As a consequence, significant structural settlements and tilts are observed during the strong earthquake [25]. The OWTs are sensitive to tilting failures due to the earthquake caused large dynamic overturning moments. The DNV standard for designing the OWT determines that the tolerance for the total rotation at seabed for pile foundation is 0.5° [16]. Currently, there is no well-calibrated design method for assessing the seismic performance of the combined OWT system with superstructure, foundation, and surrounding soil. The seismic stability design mainly refers to the standard for onshore wind turbines and local buildings [26, 27]. However, the OWTs are light-weight structure and installed in saturated soil, which has a significant difference from the onshore structure. The current design procedure may misrepresent the soil structure interactions (SSIs) and largely underestimate the consequence of an earthquake hazard. Therefore, investigations of seismic response of OWTs by considering the ground motion characteristics, free-field responses, local soil conditions, and SSIs are important.

Several studies have been conducted to investigate the seismic response of the OWT. De Risi and Bhattacharya [28] build a set of finite element models to evaluate the seismic assessment of OWTs with steel monopile foundation by considering several important influence factors. Dong [29] records the long-term in-situ data of an OWT in order to study the structural vibration characteristics and operational modal analysis. Hanler [30] presents a simulation method in analyzing the dynamic vibration of wind turbines by considering the ground motion. Zhang [31] performed a series of numerical analysis to study the dynamic response of an OWT as well as the liquefaction of the surrounding soil. A set of centrifuge tests have been performed in our laboratory to study the seismic behavior of OWTs with monopile foundation, gravity foundation, group pile foundation, and suction bucket foundation [32-35]. The monopile foundation without fixity illustrates large tilting during the earthquake, and the gravity foundation experiences the largest settlements; the surrounding soil is reinforced by the group-pile and the suction bucket foundation, and the liquefaction tendency is milder under and adjacent to the foundations. However, few open literatures describe the interaction mechanism of the seismic response. The SSIs induce cyclic inertial forces acting on the foundation, leading to structural settlements and lateral displacements [35, 36]. The foundation characteristic brings great influence on the overall dynamic response.

The friction wheel is similar to the individual shallow footings for buildings. The field investigations in the Dagupan City area after the 1990 Luzon earthquake revealed that severe settlements occurred in corner buildings without adjacent structures and in the areas that were separated from other buildings [37]. The confining effects of the structure and adjacent buildings were effective in reducing the settlement. As a reinforcing measure, the sheet pile was installed under the shallow foundation, and the method was checked by a series of shaking table tests [38]. The reinforced foundation performed well in reducing the structural settlements and lateral displacements. Therefore, the innovative hybrid monopile foundation has a great potential in enhancing the seismic stability of the OWT. The friction wheel is added at the mudline in order to provide an additional restoring moment, and hence the foundation stability is enhanced. Comparing to the single pile, the addition of the wheel increases the effective earth pressure in the underlying soil, leading to a lower tendency of soil liquefaction. During the shaking, the interactions between the pile and the wheel may reduce the shear force being transmitted to the beneath soil, and the lateral inertial forces of the foundation and the soil are different due to the structural rocking. The seismic response of the new hybrid monopile foundation is studied in this article. Moreover, the dimension of the hybrid foundation system is proved to be significant to their behaviors, and hence influences of the wheel specification are considered.

In this study, a series of centrifuge tests are performed to study the seismic response of the innovative hybrid monopile foundation under earthquake loading. The bearing mechanism of the foundation system is demonstrated by theoretical analysis. Two key parameters are studied in the tests: the wheel thickness and the wheel diameter. Following the introduction of the centrifuge test setup, the test results are presented; afterward, the influences of critical parameters and their mechanisms are discussed. The study aims to generate representative test results of the OWT with hybrid monopile foundation in earthquake events and provide design references for future

projects.

2. Application of the Hybrid Monopile Foundation

The hybrid monopile foundation is designed with the purpose of having the wider adaptability to the new generation of OWTs. The innovative foundation has features of the traditional monopile foundation and the gravity base, and hence certain existing methodologies of manufacturing, transportation, and installation can be used in the application of the hybrid monopile foundation. The monopile foundation used for the OWT is usually constructed by pipe piles with the diameter ranging from 3m to 4m and the length ranging from 20m to 35m [39]. The monopile is constructed onshore and transported to offshore sites on barges. In some cases, the large diameter monopiles are floated to the site by capping and sealing the ends. The monopile is installed by drilling and grouting, driving, and combinations of drilling and driving [40]. The jack-up rig is a fairly stable platform for installing the monopile, and the ship-shaped vessels with rotating cranes are the optimal selection in carrying out the construction [41]. The gravity base is constructed onshore and transported to the offshore site by the heavy lift vessel. During the installation, the gravity base is filled with ballast, and the positioning system is necessary to keep the stability [42]. The gravity base is cost-efficient when the dead load is high and the environmental loads are relatively low, and the seabed preparation is necessary. For larger capacity OWTs being installed in locations with larger water depths, the traditional foundations expose limitations. The diameter of the monopile may become excessively large, and the gravity base tends to reach a quite large size with a diameter of 10-20m and weight up to 2000tons [21]. In this situation, the material cost increases significantly; moreover, the substantial equipment is required for the manufacture, transportation, and installation, including jack-up barges, ship hires, and drilling equipment, etc.

The hybrid monopile foundation has shown a larger ultimate bearing capacity compared to the monopile foundation from previous researches, which can provide twice of the lateral capacity with a similar vertical load [22, 43]. The lateral resistance is the governing factor in designing the foundation supporting earth retaining structures. Therefore, the innovative foundation is promising for applications in more severe environmental conditions instead of continuously increasing the size of the traditional foundation. The pile and the wheel are expected to maintain the reasonable size. The two components can be fabricated and deployed from the existing shipyards and facilities, and the original transportation and installation equipment can be employed, which is beneficial in reducing the initial cost and realizing the innovative concept.

The installation of the hybrid monopile foundation needs investigation before applying in practicality. The hybrid monopile foundation is not only an innovative support structure for OWTs, but it is also a reinforcement of the traditional monopile with the purpose of extending its service life. In this case, the stabilizing friction wheel can be installed at the soil surface and fitted with the existing monopile or the newly installed monopile [44]. In contrast, it is suggested by researchers that for installed hybrid monopile foundation, the friction wheel may be firstly installed, which will become a guideline for locating the monopile [45]. However, this method

needs further investigations before engineering application. Besides the solid wheel, the gravel friction wheel has been proposed in our laboratory [22]. It is consist of a confining frame that filled with gravels. The frame is installed first surround the monopile, after which the gravels are filled. The filling materials are not limited to the gravel, and they can be obtained from nearby offshore locations, transported from onshore sites, and collected from proper construction wastes. The initial cost is expected to reduce significantly through this method. However, it is worth to mention that the connection method of the monopile and the friction wheel in the water is a concern during the practical installation, which will greatly influence the behavior of the foundation. The study of the hybrid monopile foundation is in the concept proof and model test stage, and thorough investigations are necessary before the practical application. Efforts should be continuously made to verify the manufacturing, transportation, and installation processes in order to provide basic data of analysis and design of the hybrid monopile foundation in the future.

3. Centrifuge Tests

Test facility

The centrifuge testing program was carried out using the 20 g-ton geotechnical centrifuge at Case Western Reserve University [46]. The effective radius of the centrifuge arm is 1.37m, and the maximum acceleration is 200g for static tests and 100g for dynamic tests. An electro-hydraulic shake table is equipped at one end of the rotation arm to generate the earthquake loading during the spin. A rigid container is fixed on the top of the shake table to hold the experimental soil and models. The maximum acceleration used in this study is 50g, representing a scaling factor of 50 for data interpretations. All the data presented in the following sections are in prototype scale using the centrifuge scaling law (Table 1) [47].

Table 1 Centrifuge Scaling Law

Parameters	Scale Factor (Model/ Prototype)
Stress	1
Strain	1
Length	1/N
Acceleration	N
Frequency	N
Time (Dynamic)	1/N
Time (Seepage)	$1/N^2$
Force	$1/N^2$
Moment of Inertia	$1/N^4$

Centrifuge modelling is an effective method to study the seismic performance of foundations in dry or saturated sands. The centrifuge realizes testing small-scale models under large gravitational acceleration, and the stress between soil particles are assumed according to the scaling law. The soil behavior greatly depends on the stress state so that the 1g laboratory test

may not accurately replicate the real behavior. Especially for the OWTs, due to lacking well-documented field tests or case studies about their seismic behavior, reliably performed physical tests are necessary. Several researchers have used centrifuge modelling to study the seismic response of foundations. Liu [25] conducted eight centrifuge tests to study the seismic performance of shallow foundations during the earthquake, and the mechanism of liquefaction-induced settlement was investigated. Kulasingam [48] conducted twelve dynamic centrifuge model tests to investigate the liquefaction behavior of saturated sand slope by considering a range of initial relative densities and three ground motions.

The rigid container fixed inside the centrifuge has an internal dimension of 26.7m (length) × 12m (width) × 8.9m (depth). The testing soil is prepared in the container, after which the models are installed. The ground motion is applied by the shake table fixed under the container when the centrifuge spins up to 50g. The rigid walls of the container allow the shear wave to transmit from the bottom of the container as well as from the surrounding sidewalls; thereby, parts of the shear wave are likely to impart back to the testing models and intensify the applied dynamic loading. To minimize the side effect, the models are installed in the middle of the container in order to leave sufficient distances to the boundaries, and the influence is weakened in dense sand [49, 50]. The rigid container has been widely used in the dynamic centrifuge tests due to its advantages of easy construction and installation. Due to the intensified dynamic loadings, the results are more conservative and regarded as the upper bond when using rigid containers [49].

Centrifuge model

The centrifuge models are constructed with six different foundations, including a traditional single pile and five hybrid monopile foundations with variable thicknesses and diameters. The models share the same upper structure that is designed according to a 3MW OWT located at Jiangsu, China [51], and the scaling ratio between the prototype model in the centrifuge tests and the real wind turbine is 1:6. The wind tower is simulated by an aluminum rod with a length of 13m. The main purpose of this study is to investigate the soil liquefaction and SSI mechanisms during the earthquake, and hence the tower head is simplified by a lumped mass fixed on top of the wind tower. The single pile is fabricated with an aluminum rod with a diameter (d) of 1.1m and total length (l) of 7m. The hybrid monopile foundations are consist of the single pile and the friction wheel. Five hybrid monopile foundations are fabricated by considering the effects of wheel thicknesses and diameters. The detail information of the testing models is listed in Table 2. The model identification system includes: 1) foundation type (M: monopile, H: hybrid monopile foundation); 2) wheel diameter (D); 3) wheel thickness (t = 0.475m). For example, “H-D5-2t” represents the hybrid monopile foundation with a friction wheel of a diameter of 5m and a thickness of 0.95m. The testing models are depicted in Figure 2. The first group of wheels shares the same diameter of 5m but with thicknesses ranging from t to 3t; these wheels have the same contacting area with the soil, but the self-weight is different. The second group of wheels has the same thickness but different diameters, contributing different drainage lengths during the shaking. The six test models are tested in both dry and saturated conditions, and a total number of twelve centrifuge tests are performed to investigate the seismic response of the hybrid monopile

foundation.

Table 2. Detail of test models

Centrifuge model	Foundation Type	Pile dimension (m)	Wheel dimension (m)	Foundation weight (ton)
M	Monopile	d=1.1, l=7	NA	22
H-D5-3t	Hybrid monopile	d=1.1, l=7	D=5, 3t=1.425	105
H-D5-2t	Hybrid monopile	d=1.1, l=7	D=5, 2t=0.95	71
H-D5-t	Hybrid monopile	d=1.1, l=7	D=5, t=0.475	47
H-D7-2t	Hybrid monopile	d=1.1, l=7	D=7, 2t=0.95	117
H-D3-2t	Hybrid monopile	d=1.1, l=7	D=3, 2t=0.95	40

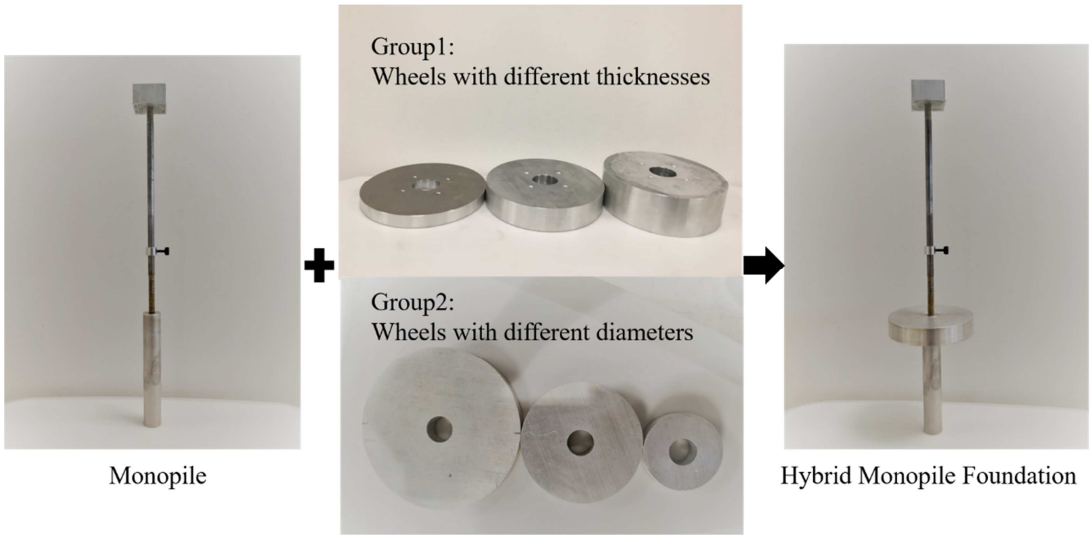

Figure 2. Test Models

Test Setup

The soil layer is constructed with Toyoura sand, which is widely used in the geotechnical investigations [32, 35, 52]. Toyoura sand is a uniform sand with angular particles, and the mechanical properties are listed in Table 3. During the soil preparations, the Toyoura sand is dry pluviated into the rigid container with a constant height, after which additional compactions are applied to obtain the desired relative density of 70% [22]. The influence of boundary conditions is less significant in dense sand. The dry tests are performed firstly to provide comparative data for the saturated condition. For the saturated sand, de-aired water was instilled slowly from the bottom of the rigid container under vacuum after preparing the dry sand, and the saturation process lasts for 24 hours. According to the centrifuge scaling law, there is a bias between the seepage time (quadratic to the scaling factor) and the test time (linear to the scaling factor) [47]. The viscous fluid is suggested by some researchers to make up this deviation [36, 53]. However, saturation is hard to attain by using the viscous fluid. This study aims to investigate the seismic performance of hybrid monopile foundations and the effects of different influence factors; thereby, for mechanism studies and model validations, the de-aired water is suggested as the pore fluid [54]. To make effective comparisons and analysis, the soil layer is newly prepared for each

centrifuge tests with the same procedures. The final thickness of the soil layer for each test is 6m, and the water elevation is 1m above the soil surface for saturated tests. After installing the centrifuge models, the monopile is fully driven into the soil layer and stands on the container bottom, simulating the pile reached bedrock in the offshore area [35, 55]; the wheels got fully contacted with the soil surface.

Table 3. Mechanical properties of Toyoura sand

Parameter	Value
C_u	1.59
C_c	0.96
Specific Gravity	2.65
D_{50}	0.17
D_{10}	0.16
Max. Void Ratio	0.98
Min. Void Ratio	0.6
Friction angle, φ	31 º

A synthetic earthquake loading is applied by the shake table fixed under the rigid container, and the shear wave is transmitted along the long side. The input ground motion is a relatively simple and strong seismic wave with one dominant frequency of 2Hz as depicted in Figure 3. This study aims to investigate the seismic performance of the innovative hybrid monopile foundation and clarify the influence factors, and hence no specific earthquake event is replicated. This input ground motion has been used in the VELACS project to study the response of a variety of models under the earthquake loading and has been used by several researchers as the "baseline" type of seismic wave [35, 56].

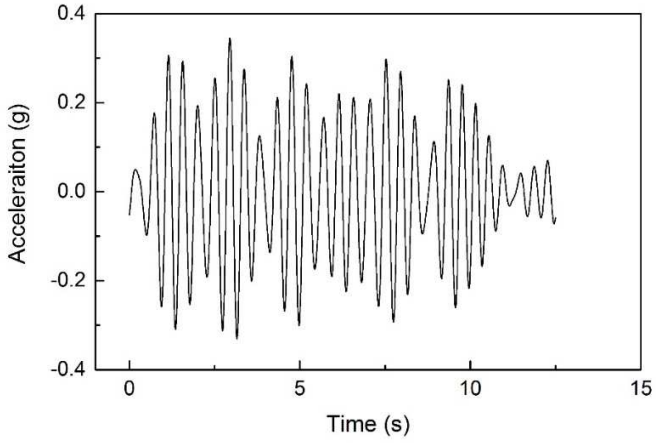

Figure 3. Input Ground Motion

The diameter of the center hole on the wheel is the same with the pile diameter. During the tests, the monopile is push-fitted through the center hole with a secure connection, and the

vertical movement between these two parts is allowed after installation. It is suggested that the hybrid foundation system is to be more effective if slight sliding is allowed between the pile and the wheel [24]. It has been proved by a series of numerical simulation that the loading capacity of the hybrid monopile foundation is not a simple algebraic summation of the capacities of a single pile and a single wheel [43]. During the lateral force, the wheel resists most of the lateral load while the pile does not play a major role in the initial stage; in the subsequent ultimate stage, the lateral resistance of the pile increases significantly and exceeds the portion of the wheel [57]. The wheel tends to rotate during the lateral load, and the bearing stress develops under the front side of the wheel reduces the bending moment in the pile. The rotation center of the wheel almost remains at the center of the wheel during the lateral load in the hybrid foundation system. The wheel is not likely to slide, and the lateral displacement is mainly caused by the pile rotation and the soil deformation. Meanwhile, the hybrid monopile foundation with a greased joint is also tested, and no big difference in the bearing capacity is observed between the smoothened and the original interface. It is assumed the change of stiffness of the joint between the pile and wheel is not considered in this study due to the limitation of the scale model. However, the connection of the two components is greatly influenced by the external loadings in a real site. The detailed analysis of the connection is necessary in the future study.

The centrifuge models are instrumented with three accelerometers (ACCs), three pore water pressure transducers (PPTs), and a linear variable displacement transducer (LVDT) to monitor the seismic performance of the soil as well as the structure. The settlements of the foundation and the soil are monitored by calipers before and after the centrifuge tests. The arrangement of the transducers is depicted in Figure 4 together with the schematic plot of the test package. The ACCs and PPTs are installed in the pair at the same depth of 1.25m but different horizontal distances to the monopile. The ACC1&PPT1 are placed next to the pile and under the wheel; the ACC2&PPT2 are installed 2.5m away from the monopile, representing the edge of the 5m diameter wheel; the ACC3&PPT3 are placed 8m away from the pile center, which monitors the seismic behavior of the free field. The measured location of the free field has sufficient distances to the container sidewall and the wheel edge in order to minimize the boundary or structural influences. The OWTs are sensitive to the tilting failures. Therefore, the LVDT is fixed at 4m above the soil surface to monitor the lateral displacement during the shaking. The ACCs are used to record the seismic response of the soil since the shear wave velocity is directly related to the soil shear modulus [58]. When the recorded accelerations maintain their shapes with the input motion during the shaking, it is demonstrated the soil keeps its strength and stiffness to allow the shear wave to be transmitted effectively. It is worth to mention that the ACCs are placed along the transmission direction of the shear wave in order to record the reliable data. In the saturated tests, the PPTs are used to monitor the soil liquefaction along with the ACCs. During the earthquake, the soil is softened due to the buildup of pore water pressure. The soil liquefies when the pore water pressure ratio (PPT ratio, defined as the ratio of excess pore water pressure to the initial effective stress $\Delta u/\sigma'$) reaches 1, at which points the soil loss its strength and stiffness. The PPT ratio decreases with the dissipation of excess pore water pressure, after which the water is squeezed out between the soil particles, and hence the soil regain its strength and stiffness. In this

case, the recorded accelerations are likely to show significant reduction since the shear wave cannot be transmitted in liquefied soil [59]. The lateral displacement and the settlement are recorded to demonstrate the seismic response of the structure. The offshore wind turbine is sensitive to the lateral failure, and the settlement should be considered by adding the friction wheel. They are important parameters in the safety assessment. As shown in Figure 3, the input ground motion lasts for 12.5s. To monitor the whole process of the seismic response, the data acquisition system starts recording 2.5s ahead of the seismic wave and keeps recording for 10s after the earthquake. In the data interpretation, the time history describes seismic the response for a total period of 25s. Detail parameters of the transducers are described by Qin [60], and the sensors are calibrated before the tests.

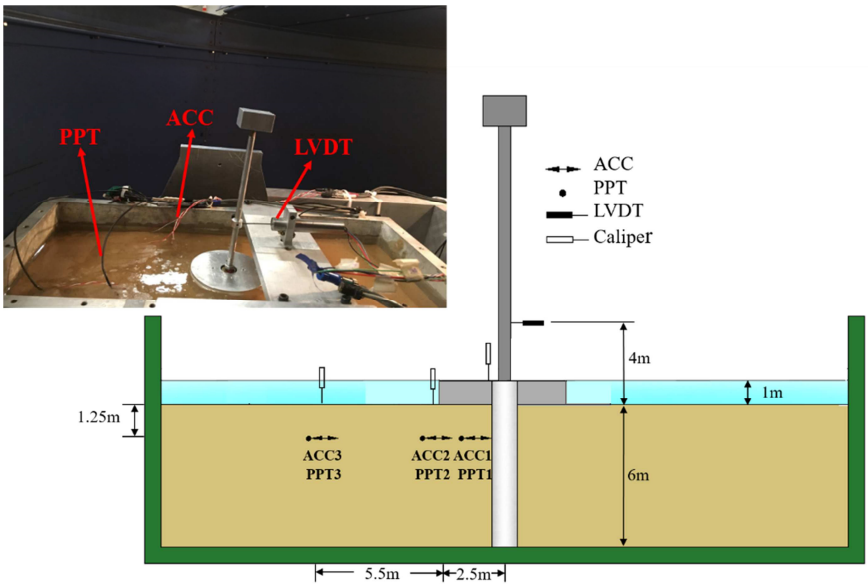

Figure 4. Test package and layout of transducers

4. Experimental Results and Findings

Results of Dry Tests

The time histories of the six models recorded during the earthquake event are plotted in Figure 5. For each model, the accelerations are recorded at three locations: near the pile (ACC1), near the edge of the wheel (ACC2), and the free field (ACC3). The acceleration time histories illustrate the similar shape and peak value of around 0.3g at three horizontal measuring locations for each model, and there are no obvious differences among the six models. During the shaking, the shear wave is transmitted effectively in the soil layer regardless of the structural influence. The accelerations do not show a severe reduction in peak values compared to the input earthquake wave. The soil maintains its strength and stiffness. The hybrid monopile foundation does not show obvious differences compared to the hybrid foundations, and different wheel dimensions are not likely to influence the seismic response of soil in the dry condition.

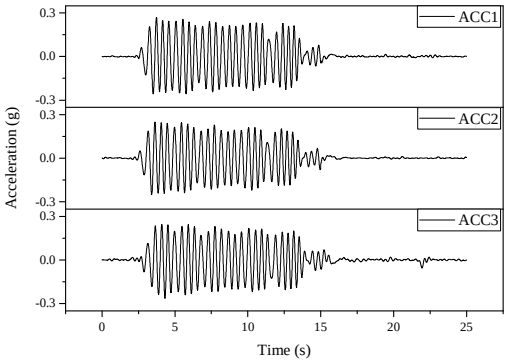

a) Model M

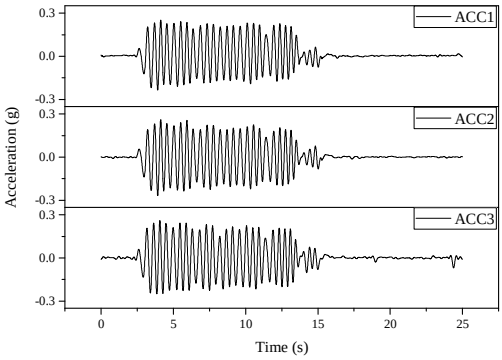

b) Model H-D5-3t

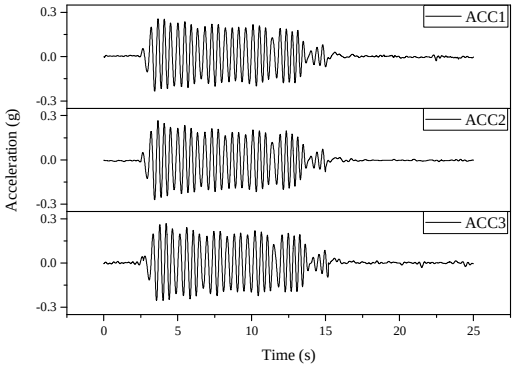

c) Model H-D5-2t

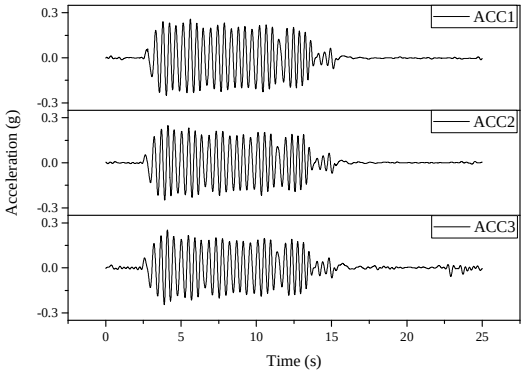

d) Model H-D5-t

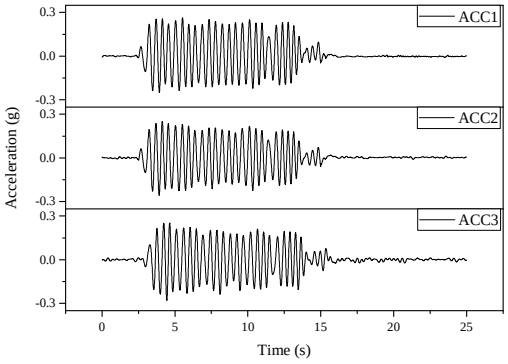

e) Model H-D7-2t

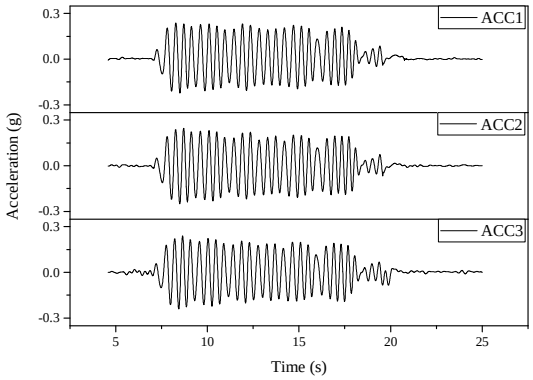

f) Model H-D3-2t

Figure 5. Time history of acceleration for dry tests

The OWT is sensitive to lateral failures during the earthquake event. Time histories of lateral displacements of the six models are recorded by an LVDT fixed on the wind tower. To clearly present the seismic response of different models, the recorded lateral displacements are plotted together in Figure 6a; Figure 6b is the zoomed version of the same test data, but with focuses on the early stage of the ground motion. Lateral displacements of the six models begin to

accumulate right after the first loading cycle, and the increasing rates are roughly linear with time. After reaching the plateau, the lateral displacements rock in small amplitudes. To be more specific, the monopile foundation experiences the largest accumulation rate during the shaking, whose lateral displacement quickly surpasses those measured from the hybrid monopile foundations. Finally, the monopile presents the largest lateral displacement. In contrast, displacements of the hybrid monopile foundations accumulate in much milder rates than the single pile, and the total deformations are smaller. The friction wheel introduces additional restoring moment to resist the static and dynamic shear stress induced by the superstructure, and the passive earth pressure acting on the embedded part of the wheel contributes more resistances to the lateral failure [43]. The hybrid monopile foundations demonstrate better lateral stabilities during the earthquake event.

The seismic response of the OWT is greatly influenced by the foundation characteristics. In the zoomed time histories of lateral displacement, the five hybrid foundations present similar oscillations with small deformations initially, and they demonstrate different increasing rates and peak values afterward. The H-D7-2t model, having the largest diameter and weight, attains the smallest final displacement with a fast stabilizing rate. Meanwhile, lateral displacement of the H-D3-2t model accumulates throughout the whole shaking event, and the displacement rate reduces significantly after the end of strong shaking; finally, this model reaches the largest lateral deformation. In general, the hybrid monopile foundation with larger weight and diameter is less likely to reach lateral failure during the earthquake. Specifically, model H-D5-3t, model H-D5-2t, and model H-D5-t share the same diameter of 5m, but they have a range of thicknesses of t to 3t. These three models have the same contacting area with soil, and the weight is the dominant control factor to influence their lateral deformations. As expected, the thicker plate leads to smaller lateral displacement, and it reaches the plateau faster. The model H-D7-2t, H-D5-2t, and H-D3-2t having the same thickness but different diameters, demonstrate more obvious gaps of their final lateral displacements. Besides the weight effect, the influence of diameter is involved. The increased contacting area leads to larger restoring moments provided by the soil bearing stress.

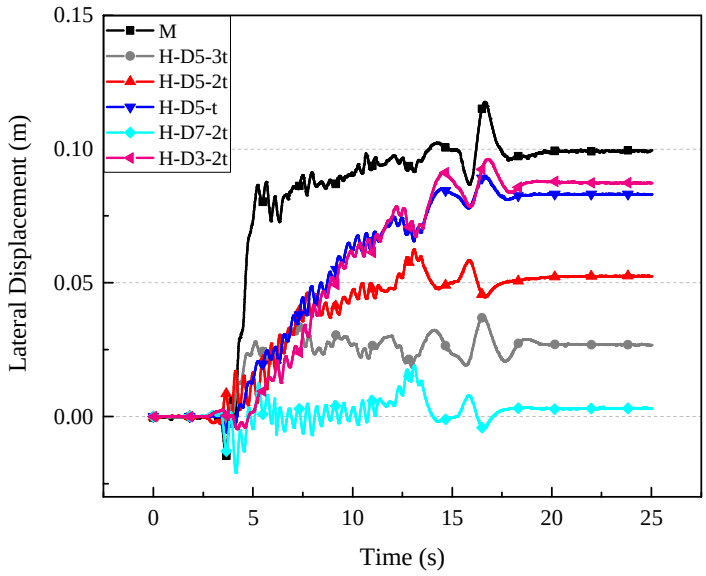

a) Time history

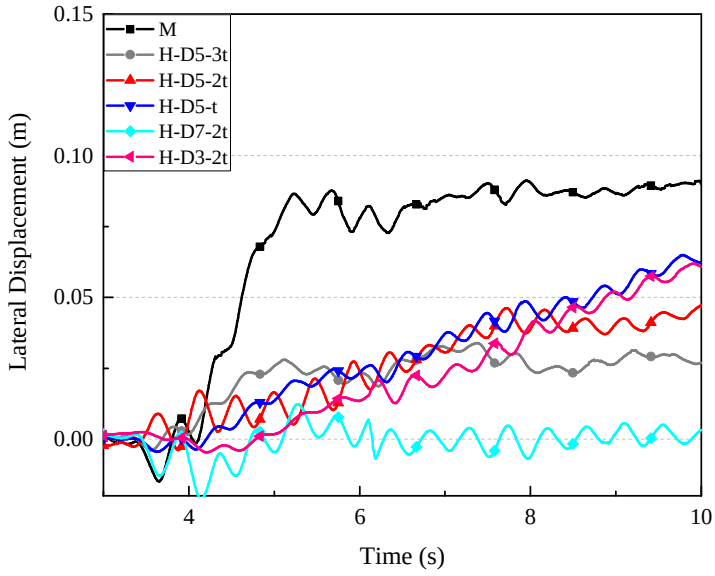

b) Zoomed time history

Figure 6. Time history of lateral displacement for dry tests

Settlements of the six models are measured at the three locations mentioned above before and after the tests as listed in Table 4. Without the friction wheel, the measurement of the monopile at location 1 is the settlement of the soil surface. In the free field where the structural influence and boundary effects are minimized, the settlements are similar for all the test models. In the dry condition that no drainage occurs, the settlement mainly attributes to the soil densification and rearrangement of soil particles. At the other two locations, settlements of the

hybrid foundations are obviously larger than the monopile due to the SSI-induced static and cyclic loading of the foundation. As a result, the settlement measured around the monopile is less than half of the hybrid foundations. The soil under the static shear stress imposed by the wheel as well as the superstructure is likely to deform horizontally away from the underneath the foundation. Meanwhile, the cyclic shear stress around the foundation results in the cumulative settlements. As demonstrated in the acceleration histories, the soil maintains its strength during the shaking, and hence the settlements are relatively small. By comparing the settlement of different hybrid foundation models, there is a tendency that the heavier hybrid foundation produces a larger settlement. The heavier structure experiences larger static or cyclic shear stresses and moments, which intensify the deformation. For similar weights, the larger diameter wheel tends to reduce the SSI-induced settlement due to the less rocking; however, this phenomenon is not obvious in the dry tests, and the weight is the dominant influence factor.

Table 4. Settlements of dry tests

Model ID.	Foundation Location 1 (m)	Soil Surface 2.5m From Foundation Location 2 (m)	Free Field Location 3 (m)
M	0.070	0.070	0.050
H-D5-3t	0.190	0.175	0.070
H-D5-2t	0.175	0.150	0.065
H-D5-t	0.155	0.135	0.040
H-D7-2t	0.205	0.210	0.055
H-D3-2t	0.145	0.140	0.045

Results of Saturated Tests

In the saturated tests, generation of excess pore water pressures complicates the soil response and the SSI. The ground, as well as the structural performance, are closely monitored by ACCs, PPTs, and the LVDT, thereby giving insight into the ground failure mechanism and the impacts on the structures. The results for dry and saturated tests are plotted together to demonstrate the effect of fluid. The monopile and one hybrid model (H-D5-3t) are selected as representatives. In the plot of acceleration time history, there is a tendency that the peak accelerations of the saturated tests are much smaller than the dry tests, especially for the monopile foundation. In the saturated tests, the soil particles try to squeeze the water between them, leading in an increase of the pore water pressure. As a result, the effective stress in soil decreases, and the strength and stiffness of the soil reduces due to the excess pore water pressure. The softened soil is not a good media for the transmission of cyclic shear waves since the shear modulus is much smaller. Therefore, the recorded accelerations are significantly weakened compared in the saturated tests compared to the input ground motion as well as the dry tests. Meanwhile, the recorded lateral displacements in saturated tests are significantly larger than the dry tests. The lateral supports provided by the softened soil decreases. The generation of the excess pore water pressure also intensifies the settlements as shown in Table 5. Consequently, with the introduction of the pore fluid, the soil tends to loss its strength and stiffness, and the damages caused by the earthquake are intensified for both of the monopile foundation and the hybrid monopile.

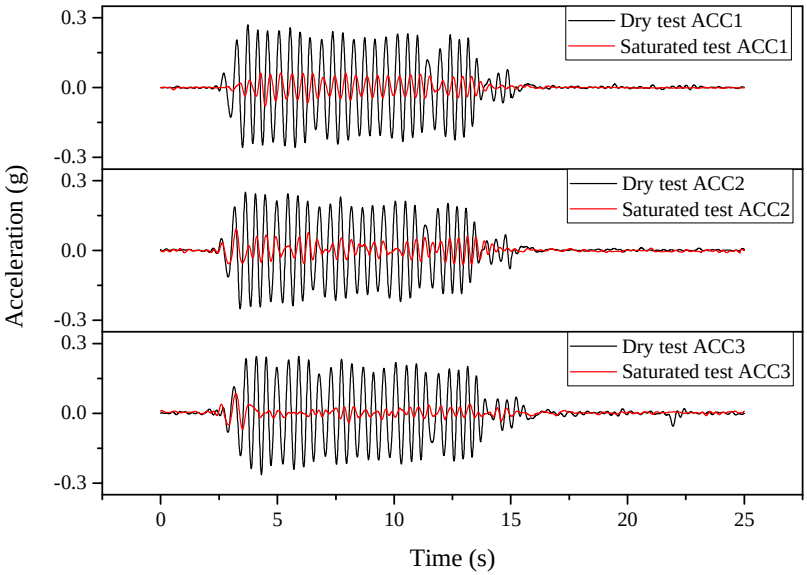

a) Time history of acceleration

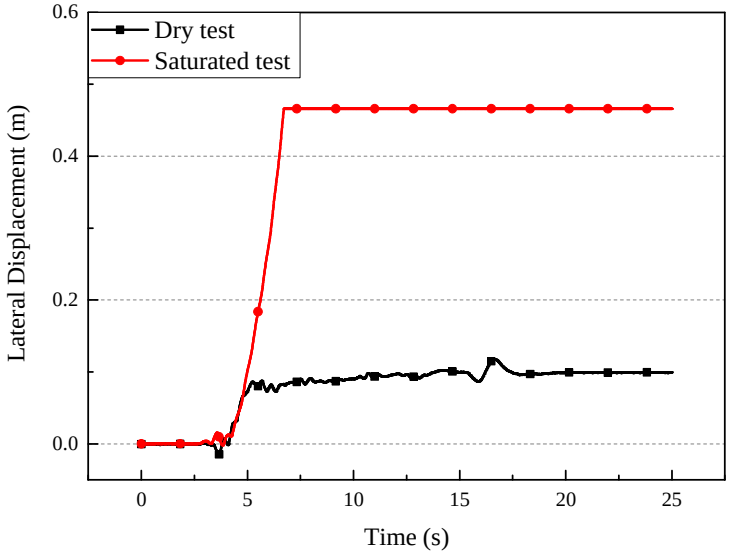

b) Time history of lateral displacement

Figure 7. Comparison of Monopile between dry and saturated test

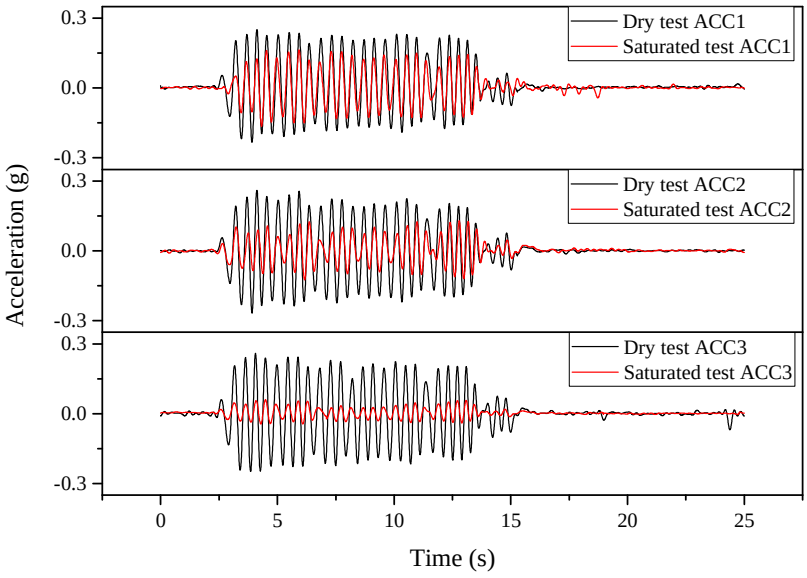

a) Time history of acceleration

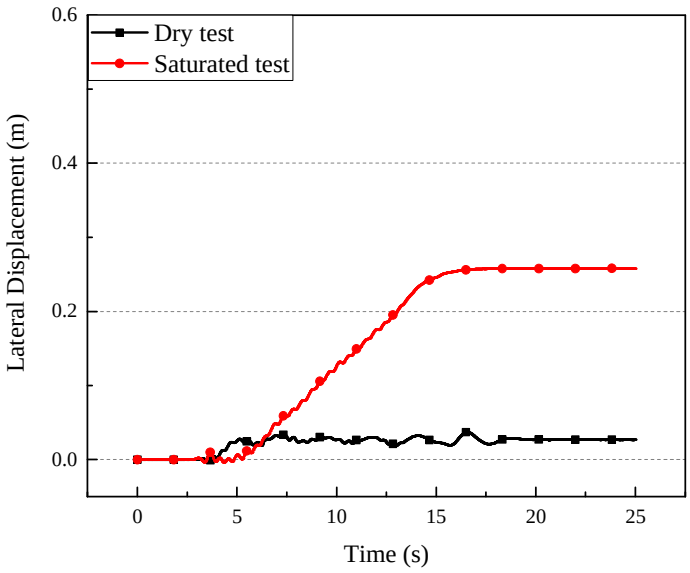

b) Time history of lateral displacement

Figure 8. Comparison of Hybrid Monopile (H-D5-3t) between dry and saturated test

Table 5. Comparison of settlement between dry and saturated test

Measuring location	Monopile		Hybrid Monopile (H-D5-3t)	
	Dry test (m)	Saturated test (m)	Dry test (m)	Saturated test (m)
Foundation (location 1)	0.070	0.105	0.190	0.265

Soil Surface 2.5m From Foundation (Location 2)	0.070	0.120	0.175	0.235
Free Field (Location 3)	0.050	0.115	0.070	0.110

Figure 9 describes the time histories of the excess pore water pressure ratio recorded for the six models during the earthquake event, demonstrating the generation and dissipation of excess pore water pressures under the foundation, near the foundation, and in the free field. The excess pore water pressures increase fast after the earthquake excitation and maintain their peak values to the end of the strong shaking; afterward, the excess pore water pressures reduce at different rates due to the influences of the wheel specification. The soil does liquefy when the pore water pressure ratio reaches 1, at which moment the soil totally loses its bearing capacity. Figure 10 shows the time histories recorded by the ACCs that are installed in pair with the PPTs. The ACCs help monitor the soil response corresponded with the PPTs.

In the free field, the pore water pressure ratio for all the models reach 1 during the shaking, representing the soil liquefaction occurs at the location 3 without disturbances of the structure. The records of ACC3 in the tests reinforce the phenomenon; the time histories of accelerations reduce obviously compared to the ground motion with a much smaller peak value of less than 0.1g. In contrast, the soil response monitored at the other two locations demonstrate significantly different tendencies. The degree of excess pore water pressure generation is greatly influenced by the confining pressure and the superstructure induced static and dynamic shear stresses. The level of soil softening and the direction of flow dissipation are affected by the foundation characteristics. For the monopile foundation, PPT1 and PPT2 show similar shapes and peak values with PPT3, demonstrating the occurrence of liquefaction around the pile. Meanwhile, the acceleration histories at three locations show analogous shapes with significant reduction. The single pile has little influence on its surrounding soil so that the ground failure mode is similar to the free field. For the hybrid monopile foundations, the pore water pressure ratios around the foundations are much smaller than the free field as depicted in Figure 9b-9f, and the liquefaction tendency is even lower near the pile (location 1) than the edge of the foundation (locations 2). The wheel introduces higher confining pressure to the soil layer, and hence the sand's strength and its resistance to pore water pressure generation are enhanced. The shaking is not strong enough to overcome this higher resistance. The recordings of ACC1 and ACC2 for the hybrid foundations agree with the conclusion from the recording of PPTs. The reductions in accelerations are much less intense than that in the free field, especially the ACC1 with a leak value of 0.15g. The soil does not liquefy under or near the hybrid foundations during the earthquake. Consequently, the hybrid monopile foundation is beneficial in reducing the liquefaction of the underneath soil, demonstrating a better seismic stability compared to the original monopile.

The pore water pressure ratio and liquefaction tendency are lower around the foundation, but the dissipation rate of excess pore water pressure is slower at these locations compared to the free field. It is assumed the seismic response of saturated sand is fully undrained during the earthquake, however, this design procedure ignores significant mechanisms and misrepresents

the consequence of liquefaction [61]. The partial drainage is proved to occur at the same time as the generation of excess pore water pressure, and the dissipation took place in a 3-D manner in response to the transient hydraulic gradient [25]. During the shaking, large hydraulic gradients form vertically upwards to the ground surface and horizontally away from the foundation. However, upwards vertical pore water pressure dissipation is slower due to the confinement of the wheel, and hence the pore pressure tends to stabilize horizontally. After the strong shaking, the PPT ratio reduces since no significant excess pore water pressures are generated and the 3-D hydraulic gradient is near the peak value. A large lateral water flow is formed under the wheel towards to free field, but the vertical dissipation is less intense. Therefore, it takes longer time for the excess pore water pressure to dissipate under or near the foundation. Moreover, it is observed that the PPT1 dissipates faster than the PPT2, and hence the soil under the wheel regain its strength faster than the adjacent soil. The pore water pressure ratio is smaller under the wheel but the absolute value of the excess pore water pressure is higher due to the higher confining pressure, and hence the horizontal water flow is from PPT1 to PPT2, which leads to more excess pore water pressures are retained at the location 2.

The characteristics of hybrid foundations have great influences on the seismic response of soil under and around the structures. For model H-D5-3t, model H-D5-2t, and model H-D5-t, the recorded ratios of PPT1 and PPT2 tend to decrease with the increase of wheel thickness. The models share the same diameter, and the dominant influence factor is weight. A growth of the foundation weight is synonymous to an increase of the contact pressure acting on the soil layer for the same contacting area. The soil is reinforced by the foundation. For the same ground motion, the soil has better ability to keep the strength and stiffness in response to the increasing confining pressure. By comparing the model H-D7-2t, H-D5-2t, and H-D3-2t, the weight is not the only consideration, and the wheel diameter is also influential. The large diameter hybrid foundation is likely to attain a smaller pore water pressure ratio but slower dissipation rate. The larger wheel reduces the ability for the seismic-induced pore water pressure to dissipate rapidly from underneath the foundation. The lateral flow forms under the foundation and moves towards the free field; thereby, the larger diameter wheel leads to longer drainage path for the dissipation, and more excess pore water pressures are sustained under the structure. The larger wheel has a larger contacting area with the soil layer. It is hard to push soil outwards of the longer path to accommodate the horizontal stability. Therefore, for the model H-D3-2t with the smallest diameter (Figure 9f), the excess pore water pressures dissipate at similar rates.

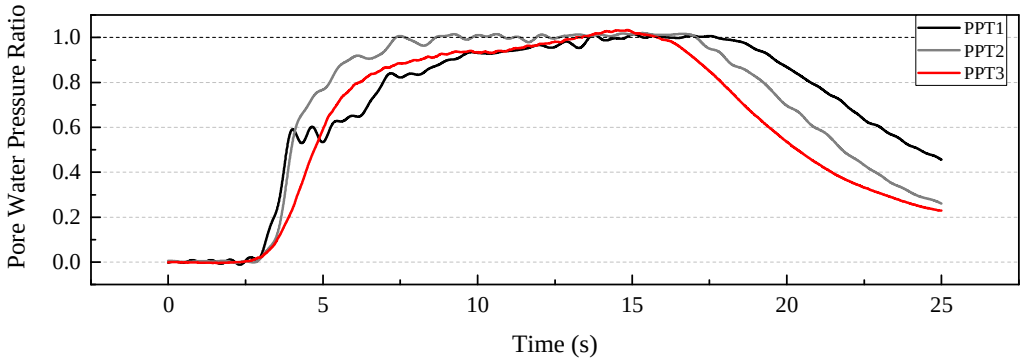

a) Model M

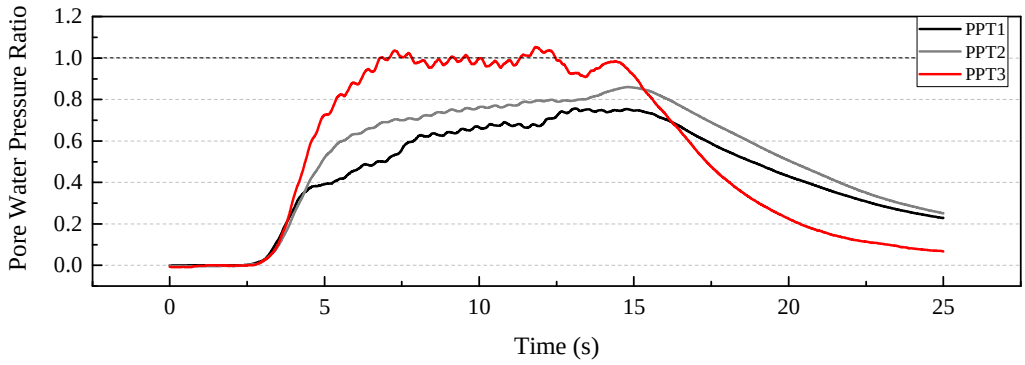

b) Model H-D5-3t

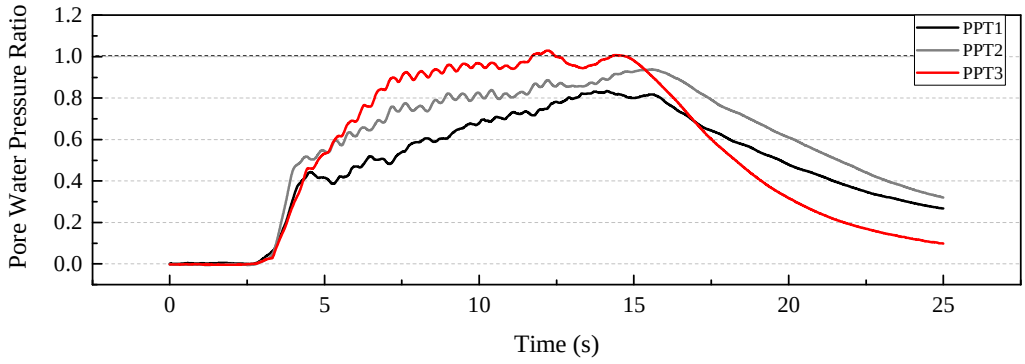

c) Model H-D5-2t

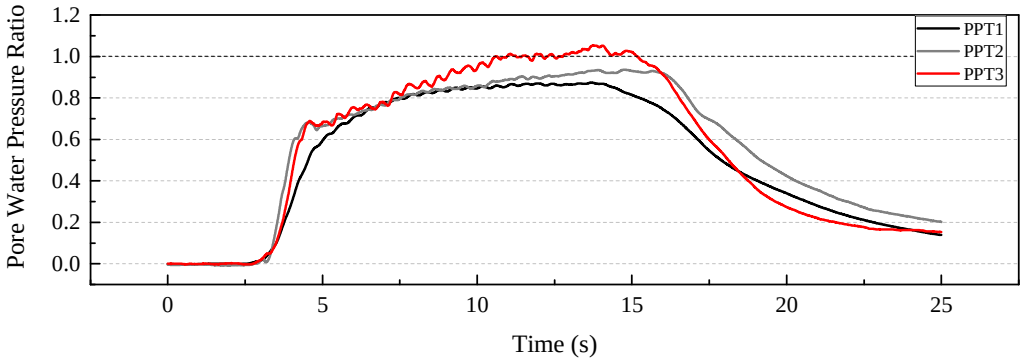

d) Model H-D5-t

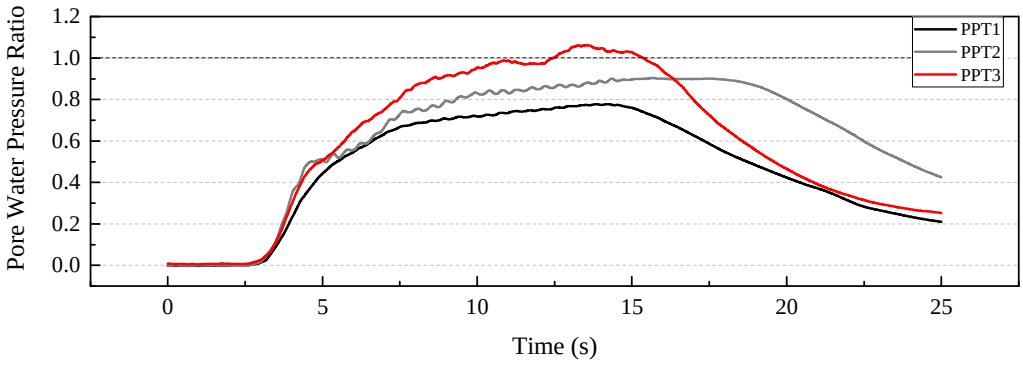

e) Model H-D7-2t

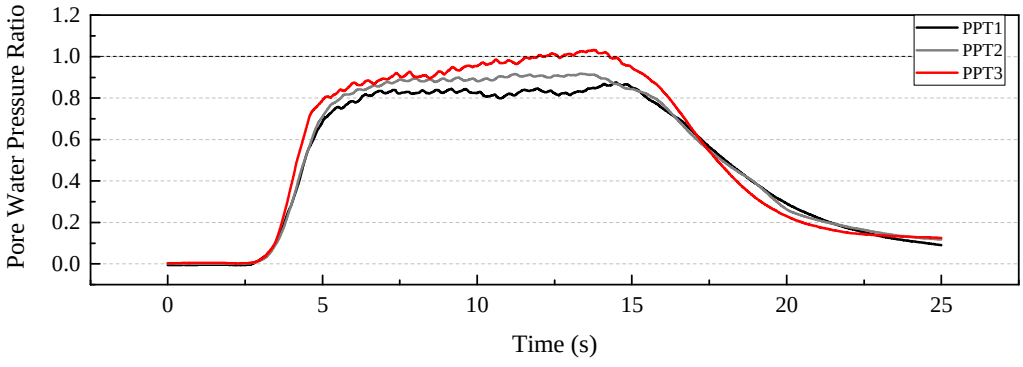

f) Model H-D3-2t

Figure 9. Time history of pore water pressure ratio for saturated tests

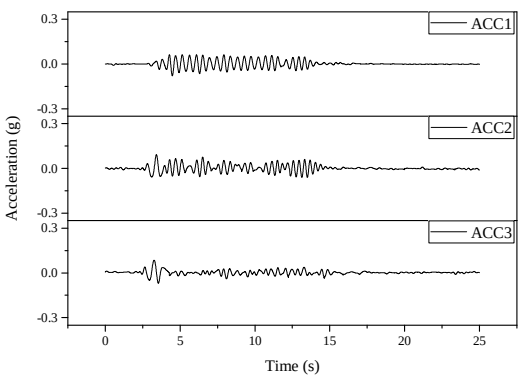

a) Model M

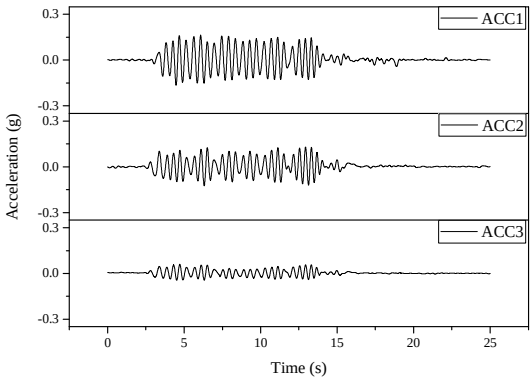

b) Model H-D5-3t

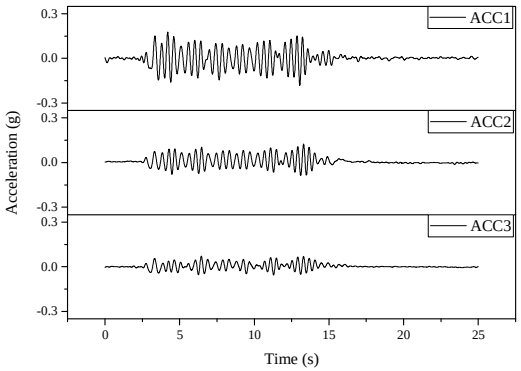

c) Model H-D5-2t

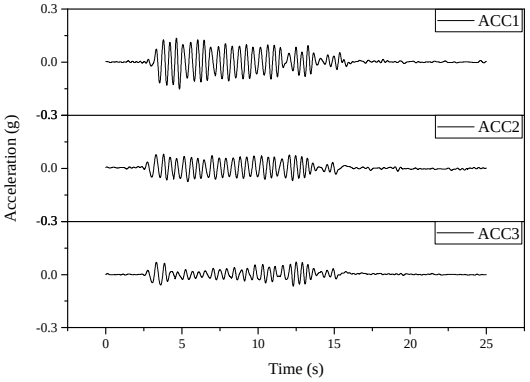

d) Model H-D5-t

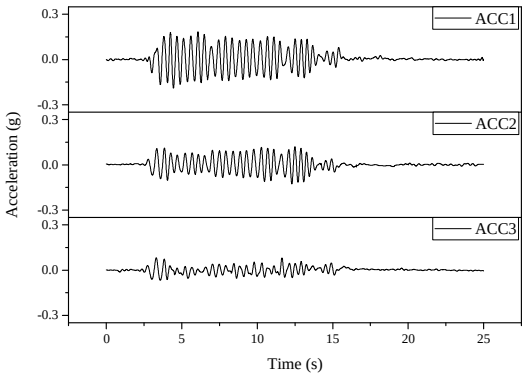

e) Model H-D7-2t

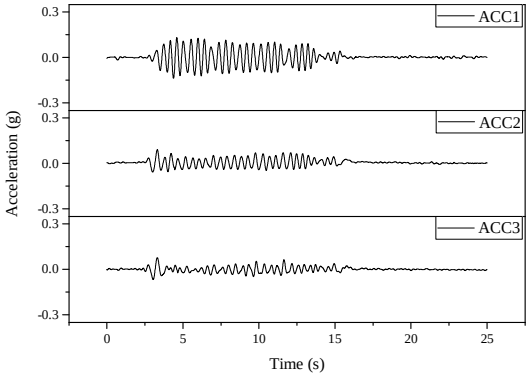

f) Model H-D3-2t

Figure 10. Time history of acceleration for saturated tests

Figure 11a depicts the time histories of the lateral displacement recorded in the saturated tests. The results of the six models are plotted together, and the zoomed time histories are presented in Figure 11b with the focus of the early stage of the excitation. The lateral

displacements accumulate in linear relationships with time but with obviously different increasing rates. The monopile foundation reaches the recording limitation quickly, indicating the happening of tilt failure. For the hybrid monopile foundations, the model H-D5-3t and model H-D7-2t attain much smaller lateral deformation than the other models, and the accumulation rates reduce dramatically at the end of the shaking. All the lateral displacements are much larger than their corresponded dry tests. In the saturated tests, the generation of pore water pressure softens the soil with or without the liquefaction, and hence the lateral support provided by the soil beneath the foundation is smaller. The zoomed time histories of the lateral displacement demonstrate that the displacements are similar at the initial stage before 4.5s for the six models. Referring to Figure 9, the excess pore water pressures have not reached their peak values, and the soil is strong enough to support the structure in this early stage. Afterward, the soil loses more bearing capacity, and the influence of foundation characteristics turns to be more intense. The monopile foundation reaches lateral failure at the largest accumulation rate, which is obviously faster than the hybrid monopile foundations. Without the reinforcement of the friction wheel, the soil around pile loses its strength quickly during the earthquake. In contrast, the accumulation rate for the hybrid foundations is much milder. The wheel provides extra restoring moments to the monopile foundation and reinforces the soil beneath the wheel. For the hybrid foundation, the heavier and larger diameter wheels leads to smaller accumulated lateral displacements. The larger contacting area is expected to increase the restoring moments and reduce the SSI induced deviatoric deformations, and the larger confining pressure provided by the heavier wheel is beneficial for reinforcing the soil.

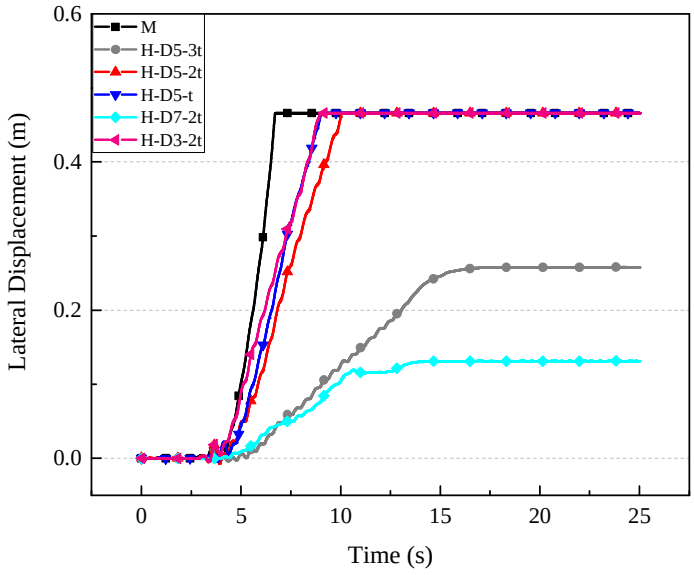

a) Time history

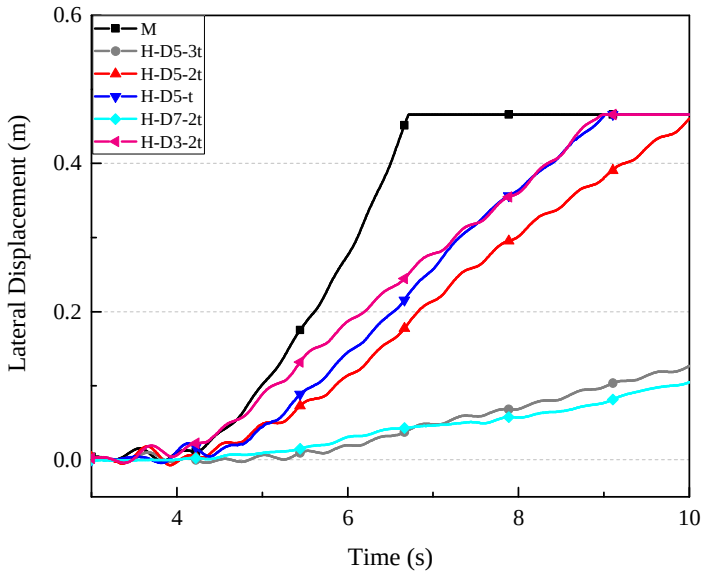

b) Zoomed time history

Figure 11. Time history of lateral displacement for saturated tests

The settlement of the six models in the saturated tests is listed in Table 6. The settlements recorded in the saturated tests are about twice of those in the dry tests. The seismically induced excess pore water pressures result in the strength loss of the soil, and hence the settlement is intensified. For the monopile foundation, the settlement measured at the free field is similar to those measured at location 1 and location 2. Without influences of the structure, these settlements mainly result from the partially drained cyclic loading, and the sedimentation and consolidation with the dissipation of excess pore water pressures. For the hybrid monopile foundations, the foundation (location 1) settles more than the adjacent ground surface (location 2), and the ground adjacent to the foundation (location 2) settles more than the free field (location 3). Although the pore water pressure ratio is lower beneath and near the hybrid foundation, the larger confining pressure leads to a higher potential for the generation of excess pore water pressure, which intensifies the settlement. The outward flow results in larger localized volumetric settlements; the structure-induced static shear stress drives the soil to deform horizontally away from the foundation; the SSI induced cyclic shear stress disturbs the underneath soil and leads to cumulative settlements. Moreover, the heavier foundation tends to cause larger settlements due to the larger stress transmitted downwards.

Table 6. Settlements of saturated tests

Test ID.	Foundation Location 1 (m)	Soil Surface 3m From Foundation Location 2 (m)	Free Field Location 3 (m)
M	0.105	0.120	0.115
H-D5-3t	0.265	0.235	0.110
H-D5-2t	0.245	0.215	0.130

H-D5-t	0.220	0.210	0.120
H-D7-2t	0.270	0.230	0.130
H-D3-2t	0.205	0.195	0.100

5. Discussions

Mechanism of the seismic response

The OWT is sensitive to tilting failure during the earthquake events. The innovative design of the hybrid monopile foundation is proved to be an effective improvement in enhancing the overall stability of the OWT as well as the surrounding soil. In the dry condition, the lateral displacement and the accumulation rate for the hybrid foundations are obviously smaller compared to the traditional monopile. In the saturated tests, the improvement is more significant. The introduction of the friction wheel reinforces the surrounding soil, leading to a higher capacity in resisting the liquefaction during the shaking. The soil beneath the foundation keeps part of its strength and stiffness to support the structure. Meanwhile, the earth pressure acting on the wheel imparts additional restoring moments to resist the dynamic overturning moment. As the consequence, the lateral displacement and its increasing rate are significantly smaller than the single pile, and the liquefaction does not occur under and near the foundation. However, the settlements of the hybrid monopile foundation and the adjacent soil are larger than that in the free field. The settlement mechanisms of the OWT during earthquake events are complex, which are greatly influenced by the structural characteristic, the generation of excess pore water pressure, and the SSI.

In the saturated condition, the generation of excess pore water pressure may produce and intensify several settlement mechanisms. The settlement caused by the earthquake is categorized into two types: the pore water pressure induced volumetric strain and the structure shear stress-induced deviatoric strain. At the beginning of an earthquake, the excess pore water pressure is generated with the shaking, and the local water starts to migrate as soon as the development of the 3-D transient hydraulic gradient. The water flow tends to move both within and out of the soil, which causes the localized volumetric strain. As the increase of excess pore water pressure, the soil experiences a significant strength loss. The upper parts of the sand particles are dispersed so that these particles are likely to accumulate at the bottom to form a solidified zone and consolidate under their own weights. This is the mechanism of the sedimentation-induced volumetric strain. It happens immediately after the strength loss and depends on the breakdown of the soil skeleton. When a continuum soil skeleton is re-formed after the sedimentation, the consolidation-induced volumetric strain occurs. The excess pore water pressure dissipates fast and the soil regains its effective stress, which enables larger contacting forces between the particles. These three types of volumetric strains occur continuously with the generation and dissipation of excess pore water pressures during the shaking, being responsible for the free field settlement in the tests. At the locations near the structure, the deviatoric strain induced settlement is critical in addition to the volumetric settlement. The friction wheel imposes extra static shear stress to the beneath ground,

intensifying the strength loss of the soil, which leads to the structural settlement and tilting. Meanwhile, the cyclic shear stress caused by the SSI results in the cumulative settlement. The vibration of the foundation influences the beneath soil cycle by cycle and displaces the weakest soil away from the foundation. This is the SSI-induced dynamic deviatoric strain. Moreover, the structural movement may cause larger excess pore water pressure to be generated under higher confining pressure regardless of the occurrence of soil liquefaction, which amplified all kinds of settlement mechanisms.

To investigate the SSI mechanisms more clearly, the forces acting on the OWT during the earthquake are schematically plotted in Figure 12. F_1 is the inertial force imposed by the superstructure, F_2 is the inertial force from the foundation, Q_1 is the shear stress sustained by the friction wheel, and Q_2 is the shear stress transmitted to the pile. The foundations settle during the shaking, and hence the earth pressure acting on the embedded part of the wheel is considered. P_p is the passive earth pressure while P_a is the active earth pressure. Therefore, the equation is:

$$F_1 + F_2 = Q_1 + Q_2 + P_p - P_a \quad (1)$$

The existing of the wheel introduced additional shear stress to resist the inertial force, and the earth pressure is in phase with and acts against the inertial force. Therefore, less inertial force is transmitted to the shear force on the pile, contributing to less overturning moments. This explains the phenomenon that the single pile experiences much larger lateral deformation than the hybrid foundations. Meanwhile, the differential inertial forces between the foundation and the ground produce the SSI-induced cyclic loading, resulting in the larger cumulative settlements. Therefore, the settlement of the foundation and the surrounding soil is larger than the free field as well as the monopile foundation. In the saturated condition, the soil losses part of its strength during the shaking, leading to a reduced earth pressure acting against the inertial force. Therefore, the shear stress transmitted downwards turns to be larger, and hence the settlement and tilt mechanisms are amplified.

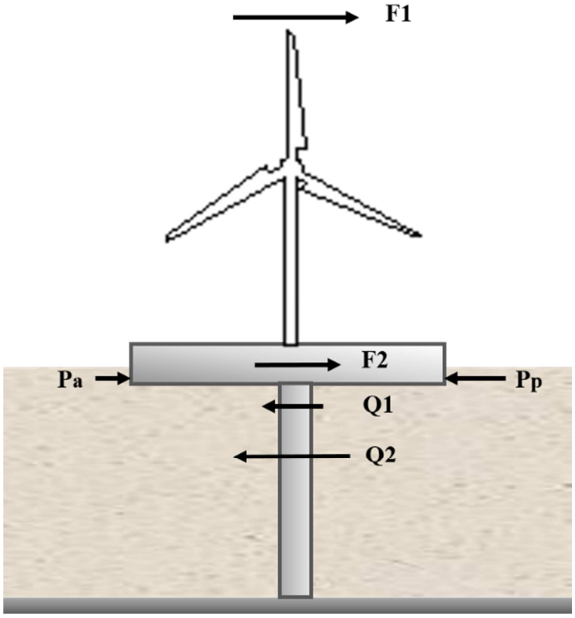

Figure 12. Schematic plot of forces acting on the OWT

Influence of wheel characteristic

The feasibility and ultimate bearing capacity of the hybrid monopile foundation have been investigated previously through the centrifuge tests [22, 43, 57]. The addition of the friction wheel is effective in improving the stability, and the bearing capacity is obviously larger than the original monopile foundation. In service conditions, the accumulated lateral deformation is smaller with the increasing number of loading cycles, and it is greatly influenced by the soil characteristic and the peak load. The ultimate bearing capacity of the hybrid monopile foundation is estimated by using the analytical method for piles, and the function of the friction wheel is simplified as an equivalent restoring moment acting at the pile head. Parametric studies have been conducted to investigate the influence of wheel thickness and diameter to the bearing capacity. The bearing capacity increases at a nearly constant rate with the increase of the wheel thickness. By increasing the wheel diameter, the bearing capacity and the initial stiffness are enhanced at an increasing gradient, and the improvement is more pronounced when the diameter is larger than 3m. In this study, assessments of the tendencies of the centrifuge test results enable a qualitative analysis of the influence of wheel characteristics on the seismic response of the hybrid monopile foundation. The assessments include effects of wheel thicknesses and diameters on the soil response, the structural lateral displacement, and the settlement.

Figure 13 depicts the influence of wheel thickness to the lateral displacement and the settlement. It is clearly shown that the displacement and settlement are much larger in the saturated condition compared to the dry condition due to the influence of pore fluid. The lateral displacement tends to decrease with the increase of wheel thickness. They are in a linear relationship in the dry sand; in the saturated tests, the hybrid foundation reaches the measuring limitation when the thickness is smaller than 1m, and the value drops significantly as the thickness increases to 3t. In contrast, the settlement tends to increase with the wheel thickness, but the changing rate is milder than the lateral displacement.

The wheels with the same diameter but different thicknesses from t to 3t represents an increase of the foundation self-weight for the same soil contacting area. In all the tests, the lateral displacement recorded during the shaking reduces significantly with the increase of the wheel weight. The wheel with larger weight is likely to provide larger shear stresses (Q_1) under the wheel, and earth pressures acting on the wheel is expected to be enhanced, which are beneficial for the structural lateral stability during the earthquake event. The larger soil bearing stress tends to provide larger restoring moments to resist the dynamic vibration. In the saturated condition, the effect of the wheel weight is more significant. The heavier wheel introduces more confining pressure to the soil layer, and hence the excess pore water pressure ratio is smaller with the increase of self-weight. However, although the liquefaction does not occur under and near the wheel, the heavier wheel enables a larger pore water pressure to be generated in the underlying soil, which intensifies several settlement mechanisms, especially the SSI induced deviatoric strains. Consequently, increasing the weight of the hybrid monopile foundation is beneficial for the lateral stability and the resistance to liquefaction, but the settlement is intensified.

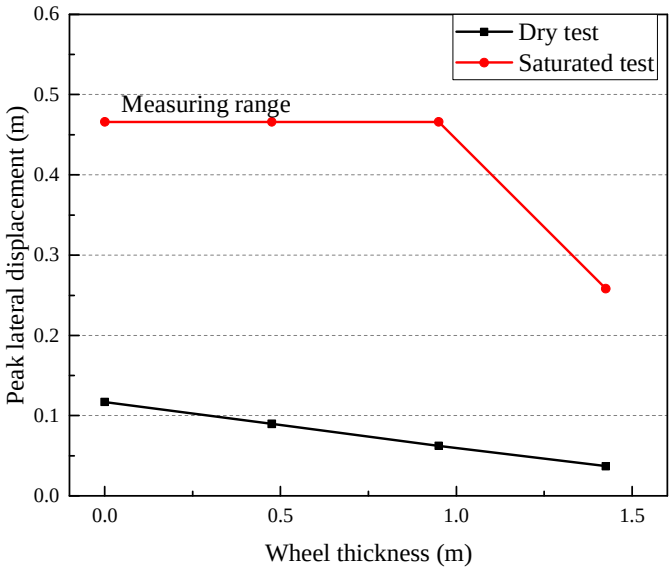

a) Influence of wheel thickness to peak lateral displacement

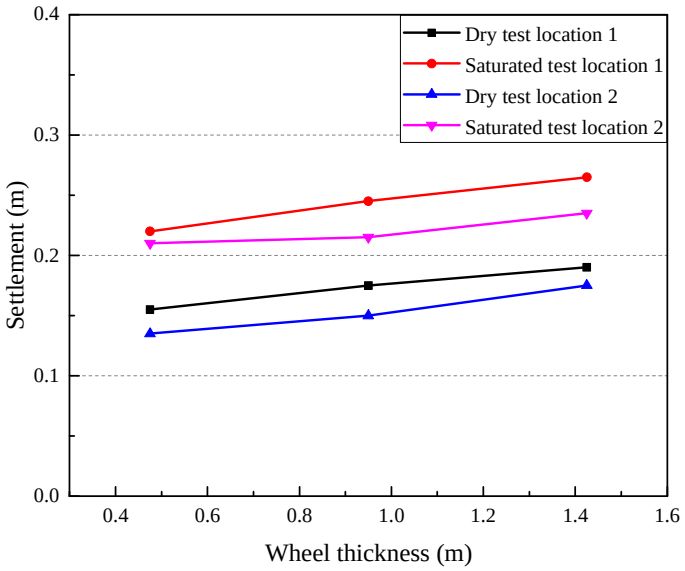

b) Influence of wheel thickness to settlement
Figure 13. Influence of wheel thickness

Besides the influence of the weight, the foundation diameter is a major factor to influence the seismic response. The influence of the wheel diameter is presented in Figure 14. The lateral displacement decreases with the increase of the wheel diameter, and the influence is more pronounced the diameter exceeds 3m in dry sand, which agrees with previous observations that the diameter of a stabilizing base is suggested to be at least 50% of the wall embedment depth to

reach optimal effects [62]. In the saturated test, the displacement reaches measuring range when the diameter is small, and it drops to 0.131m when the diameter increases to 7m.

The wheel with larger diameter results to smaller lateral deformation during the earthquake event. The larger wheel leads to a higher capacity in a larger volume of soil under and around the foundation, and hence the moment resistance is higher, which helps to resist the lateral failures. In the saturated soil, the larger diameter wheel results in bring longer drainage path. The dissipation of excess pore water pressure requires a longer pathway, and hence more excess pore water pressures are sustained under the foundation. Therefore, it takes longer time for the excess pore water pressure ratio to decrease for larger diameter foundations. The feature of the pore water pressure influences the main settlement mechanisms. The initial localized volumetric strains due to the partial drainage are reduced, but the contribution of sedimentation and consolidation strains are likely to be amplified due to the broader impact of soil skeleton and larger hydraulic gradient. The static deviatoric strain increases due to the immediate settlement procedure. The SSI-induced cyclic deviatoric strain is expected to decrease since the foundation rocks less with a larger diameter. The cyclic shear stress may not be large enough to push soil to a larger distance. With the same weight, the hybrid monopile foundation settles less with the increase of wheel diameter, and this result agrees with the previous studies [63].

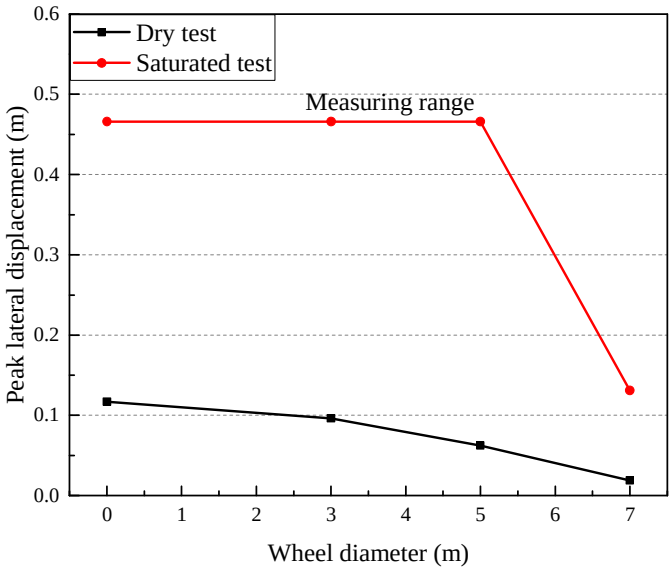

a) Influence of wheel diameter to peak lateral displacement

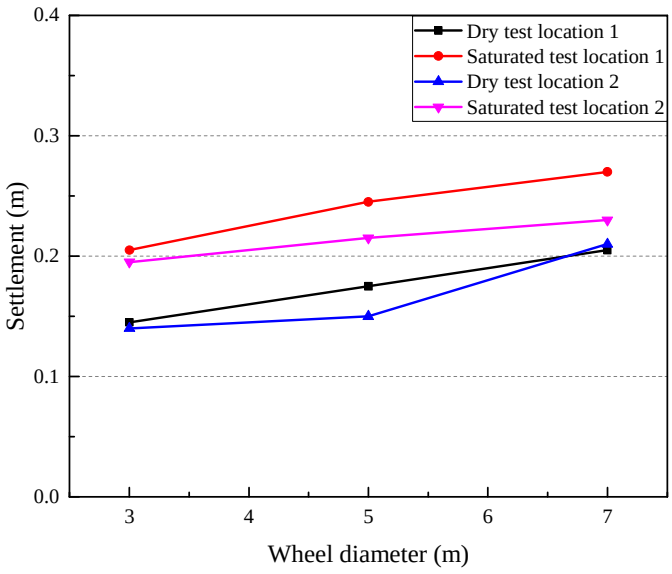

b) Influence of wheel diameter to settlement
Figure 14. Influence of wheel diameter

6. Conclusions

In this study, a series of centrifuge tests are performed to study the mechanism of seismic response of OWT with the innovative hybrid monopile foundation. Six models are tested in the sandy soil, including one traditional monopile and five hybrid foundations with variable diameters and thicknesses. The seismic response of soil and the structure is monitored by accelerometers, pore water pressure transducers, and LVDTs during the tests, and the settlement is measured by the caliper. Dominant mechanisms of the ground shaking induced seismic behavior are identified, and the impact of the influence factors are summarized. The following conclusions are drawn according to the centrifuge tests and the mechanism analysis:

1) The monopile foundation experiences large tilt during the earthquake. The hybrid monopile foundations attain much smaller lateral deformations as well as the accumulation rate. The soil bearing capacity is improved by the wheel-induced higher confining pressure. The introduction of the wheel provides an additional restoring moment to enhance the structural lateral stability, which is the dominant failure mode for the offshore wind turbine.

2) The settlement of the hybrid monopile foundation is more significant than the free field due to the SSI-induce static and cyclic shear stress. In the saturated condition, the generation and dissipation of excess pore water pressures intensify several settlement mechanisms, including both the volumetric strain and the deviatoric strain around the structure.

3) Dry sand can provide sufficient bearing during the shaking, and the soil keeps its strength to resist the structural failure.

4) The structural lateral displacements and settlements are more intense in the saturated tests compared to the dry tests. The soil behavior is largely influenced by the excess pore water

pressure. The liquefaction does occur around the monopile foundation and in the free field. The pore water pressure ratios are significantly reduced under and adjacent to the hybrid foundation due to the wheel-induced confining pressure. The soil around the foundation keeps part of its strength and stiffness during the earthquake event.

5) The hybrid foundation with larger weight tends to have smaller lateral displacement and lead to a smaller tendency of liquefaction during the shaking, but the settlement is larger due to the more intense soil-structure interactions. With a similar weight, the hybrid monopile foundation settles less with the increase of wheel diameter, and the lateral stability is expected to be enhanced.

Overall, this study provides well-documented test results to help expand our understanding of hybrid monopile foundation in the hazards event and facilitate the application of this innovative foundation. The hybrid monopile foundation is a new concept, and detail analysis of the manufacturing and installation will be conducted in the future.

Acknowledgment:
The information, data, or work presented herein was funded in part by the Office of Energy Efficiency and Renewable Energy (EERE), U.S. Department of Energy, under Award Number DE‐EE0006714.

REFERENCES

[1] Li J, Wang X, Yu X. Use of spatio-temporal calibrated wind shear model to improve accuracy of wind resource assessment. Applied Energy. 2018;213:469-85.

[2] Kaldellis J, Apostolou D, Kapsali M, Kondili E. Environmental and social footprint of offshore wind energy. Comparison with onshore counterpart. Renewable energy. 2016;92:543-56.

[3] Li J, Yu X. Onshore and offshore wind energy potential assessment near Lake Erie shoreline: A spatial and temporal analysis. Energy. 2018;147:1092-107.

[4] Feng J, Shen WZ. Design optimization of offshore wind farms with multiple types of wind turbines. Applied Energy. 2017;205:1283-97.

[5] Sklenicka P, Zouhar J. Predicting the visual impact of onshore wind farms via landscape indices: A method for objectivizing planning and decision processes. Applied Energy. 2018;209:445-54.

[6] Wang X, Zeng X, Li J, Yang X, Wang H. A Review on Recent Advancements of Substructures for Offshore Wind Turbines. Energy Conversion and Management. 2018;158C:103-19.

[7] Hou P, Enevoldsen P, Hu W, Chen C, Chen Z. Offshore wind farm repowering optimization. Applied Energy. 2017;208:834-44.

[8] Li J, Yu XB. Analyses of the Extensible Blade in Improving Wind Energy Production at Sites with Low-Class Wind Resource. Energies. 2017;10:1295.

[9] Chen J, Wang F, Stelson KA. A mathematical approach to minimizing the cost of energy for large utility wind turbines. Applied Energy. 2018;228:1413-22.

[10] González JS, Payán MB, Santos JMR. Optimal design of neighbouring offshore wind farms: A co-evolutionary approach. Applied energy. 2018;209:140-52.

[11] Europe W. The European offshore wind industry—Key trends and statistics 2017. Wind Europe: Brussels, Belgium. 2018:38.
[12] Zhu B, Byrne B, Houlsby G. Long-term lateral cyclic response of suction caisson foundations in sand. Journal of geotechnical and geoenvironmental engineering. 2012;139:73-83.
[13] Gentils T, Wang L, Kolios A. Integrated structural optimisation of offshore wind turbine support structures based on finite element analysis and genetic algorithm. Applied Energy. 2017;199:187-204.
[14] Wang X, Yang X, Zeng X. Centrifuge modeling of lateral bearing behavior of offshore wind turbine with suction bucket foundation in sand. Ocean Engineering. 2017;139:140-51.
[15] Byrne B, Houlsby G. Assessing novel foundation options for offshore wind turbines. World maritime technology conference: London:[sn]; 2006.
[16] Veritas DN. Design of offshore wind turbine structures. Offshore Standard DNV-OS-J101. 2004;6:2004.
[17] Perez-Collazo C, Greaves D, Iglesias G. A review of combined wave and offshore wind energy. Renewable and Sustainable Energy Reviews. 2015;42:141-53.
[18] Mokwa RL, Duncan JM. Rotational restraint of pile caps during lateral loading. Journal of geotechnical and geoenvironmental engineering. 2003;129:829-37.
[19] Powrie W, Daly M. Centrifuge modelling of embedded retaining walls with stabilising bases. Geotechnique. 2007;57:485-97.
[20] Wang X, Zeng X, Li J. Assessment of bearing capacity of axially loaded monopiles based on centrifuge tests. Ocean Engineering. 2018;167:357-68.
[21] Wang X, Zeng X, Li X, Li J. Investigation on Offshore Wind Turbine with an Innovative Hybrid Monopile Foundation: An Experimental Based Study. Renewable energy. 2018.
[22] Wang X, Zeng X, Yang X, Li J. Feasibility study of offshore wind turbines with hybrid monopile foundation based on centrifuge modeling. Applied Energy. 2018;209:127-39.
[23] Lehane B, Powrie W, Doherty J. Centrifuge model tests on piled footings in clay for offshore wind turbines. Proceedings of International Conference in Physical Modelling in Geotechnics, ICPMG2010 Rotterdam: Balkema2010.
[24] Arshi H, Stone K, Vaziri M, Newson T, El-Marassi M, Taylor R, Goodey, RJ. Modelling of monopile-footing foundation system for offshore structures in cohesionless soils. Proc 18th ICSMGE. 2013.
[25] Liu L, Dobry R. Seismic response of shallow foundation on liquefiable sand. Journal of geotechnical and geoenvironmental engineering. 1997;123:557-67.
[26] RP2A-LRFD A. Recommended Practice for Planning, Designing and Constructing Fixed Offshore Platforms-Load'and Resistance Factor Design. American Petroleum Institute, Washington. 1993.
[27] EUROCODE N. 8: Design provisions for earthquake resistance of structures. Part. 1994;2:1998-2.
[28] De Risi R, Bhattacharya S, Goda K. Seismic performance assessment of monopile-supported offshore wind turbines using unscaled natural earthquake records. Soil Dynamics and Earthquake Engineering. 2018;109:154-72.
[29] Dong X, Lian J, Wang H, Yu T, Zhao Y. Structural vibration monitoring and operational modal analysis of offshore wind turbine structure. Ocean Engineering. 2018;150:280-97.
[30] Haenler M, Ritschel U, Warnke I. Systematic modelling of wind turbine dynamics and earthquake loads on wind turbines. European Wind Energy Conference and Exhibition: Citeseer; 2006. p. 1-6.
[31] Zhang P, Ding H, Le C. Seismic response of large-scale prestressed concrete bucket foundation for offshore wind turbines. Journal of Renewable and Sustainable Energy. 2014;6:013127.

[32] Wang X, Yang X, Zeng X. Seismic centrifuge modelling of suction bucket foundation for offshore wind turbine. Renewable energy. 2017;114:1013-22.
[33] Wang X, Zeng X, Yu H, Lian J. Simulation of Dynamic Response of Offshore Wind Turbine with Group-Pile Foundation Using Centrifuge Tests. IFCEE 2015. p. 1781-90.
[34] Wang X, Zeng X, Yu H, Wang H. Centrifuge modeling of offshore wind turbine with bucket foundation under earthquake loading. IFCEE 20152015. p. 1741-50.
[35] Yu H, Zeng X, Li B, Lian J. Centrifuge modeling of offshore wind foundations under earthquake loading. Soil Dynamics and Earthquake Engineering. 2015;77:402-15.
[36] Dashti S, Bray JD, Pestana JM, Riemer M, Wilson D. Mechanisms of seismically induced settlement of buildings with shallow foundations on liquefiable soil. Journal of geotechnical and geoenvironmental engineering. 2009;136:151-64.
[37] Tokimatsu K, Kuwayama S, Midorikawa S, Abe A, Tamura S. Preliminary report on the geotechnical aspects of the Philippine earthquake of July 16, 1990. 1991.
[38] Chaudhary B, Hazarika H, Nishimura K. Effects of duration and acceleration level of earthquake ground motion on the behavior of unreinforced and reinforced breakwater foundation. Soil Dynamics and Earthquake Engineering. 2017;98:24-37.
[39] Bransby M, Randolph M. Combined loading of skirted foundations. Geotechnique. 1998;48:637-55.
[40] Houlsby G, Kelly R, Huxtable J, Byrne B. Field trials of suction caissons in clay for offshore wind turbine foundations. 2005.
[41] Malhotra S. Selection, design and construction of offshore wind turbine foundations. Wind turbines: InTech; 2011.
[42] Peire K, Nonneman H, Bosschem E. Gravity base foundations for the thornton bank offshore wind farm. Terra et Aqua. 2009;115:19-29.
[43] Wang X, Zeng X, Li J, Yang X. Lateral bearing capacity of hybrid monopile-friction wheel foundation for offshore wind turbines by centrifuge modelling. Ocean Engineering. 2018;148:182-92.
[44] Stone K, Newson T, Sandon J. An Investigation Of The Performance Of A'Hybrid'Monopile-Footing Foundation For Offshore Structures. OFFSHORE SITE INVESTIGATION AND GEOTECHNICS, Confronting New Challenges and Sharing Knowledge: Society of Underwater Technology; 2007.
[45] El-Marassi M. Investigation of hybrid monopile-footing foundation systems subjected to combined loading: The University of Western Ontario; 2011.
[46] Figueroa J, Saada A, Dief H, Dietz C. Development of the geotechnical centrifuge at Case Western Reserve University. Proceedings of the International Conference: Centrifuge1998. p. 3-9.
[47] Chandrasekaran V. Centrifuge modelling in earthquake geotechnical engineering. Energy. 2003;3:1.
[48] Kulasingam R, Malvick EJ, Boulanger RW, Kutter BL. Strength loss and localization at silt interlayers in slopes of liquefied sand. Journal of geotechnical and geoenvironmental engineering. 2004;130:1192-202.
[49] Yang Z, Elgamal A, Adalier K, Sharp M. Container boundary effect on seismic earth dam response in centrifuge model tests. 11th International Conference on Soil Dynamics & Earthquake Engineering and 3rd International Conference on Earthquake Geotechnical Engineering2004. p. 669-75.
[50] Takahashi H, Morikawa Y, Ichikawa E. Effects of rigid sidewall of specimen container on seismic behaviour. Physical Modelling in Geotechnics, Two Volume Set: Proceedings of the 7th International Conference on Physical Modelling in Geotechnics (ICPMG 2010), 28th June-1st July, Zurich, Switzerland: CRC Press; 2010. p. 177.

[51] Ding H, Liu Y, Zhang P, Le C. Model tests on the bearing capacity of wide-shallow composite bucket foundations for offshore wind turbines in clay. Ocean Engineering. 2015;103:114-22.
[52] Bolton M. The strength and dilatancy of sands. Geotechnique. 1986;36:65-78.
[53] Fiegel GL, Kutter BL. Liquefaction-induced lateral spreading of mildly sloping ground. Journal of geotechnical engineering. 1994;120:2236-43.
[54] ZENG X, WU J, Young B. Influence of viscous fluids on properties of sand. ASTM geotechnical testing journal. 1998;21:45-51.
[55] Tokimatsu K, Suzuki H, Sato M. Effects of inertial and kinematic interaction on seismic behavior of pile with embedded foundation. Soil Dynamics and Earthquake Engineering. 2005;25:753-62.
[56] Arulanandan K, Scott R. Project VELACS—Control test results. Journal of geotechnical engineering. 1993;119:1276-92.
[57] Yang X, Zeng X, Wang X, Yu H. Performance of monopile-friction wheel foundations under lateral loading for offshore wind turbines. Applied Ocean Research. 2018;78:14-24.
[58] Fu L, Liu G, Zeng X. Evaluation of shear wave velocity based soil liquefaction resistance criteria by centrifuge tests. Geotechnical Testing Journal. 2008;32:39-44.
[59] Su D, LI X-s. Centrifuge investigation on seismic response of single pile in liquefiable soil [J]. Chinese Journal of Geotechnical Engineering. 2006;4:000.
[60] QIN J. CENTRIFUGE MODELING THE INFLUENCE OF FABRIC ANISOTROPY ON SEISMIC RESPONSE OF FOUNDATIONS: Case Western Reserve University; 2016.
[61] Dashti S, Bray JD, Pestana JM, Riemer M, Wilson D. Centrifuge testing to evaluate and mitigate liquefaction-induced building settlement mechanisms. Journal of geotechnical and geoenvironmental engineering. 2009;136:918-29.
[62] Powrie W, Chandler R. The influence of a stabilizing platform on the performance of an embedded retaining wall: a finite element study. Geotechnique. 1998;48.
[63] Yasui M. Settlement and inclination of reinforced concrete buildings in Dagupan City due to liquefaction during the 1990 Philippine earthquake. 1992.